IEEE Workshop On Robot Vision (WorV) 2013
Clearwater Beach, Clearwater FL, USA
January 16-17, 2013

A Wireless Robotic Video Laparo-Endoscope for Minimal Invasive Surgery

Adham Alqassis[1], Cristian A. Castro[1], Sara Smith[2], Thomas Ketterl[1], Yu Sun[3], Peter P. Savage[4], and Richard D. Gitlin[1]
[1]Department of Electrical Engineering, [2]Department of Industrial Engineering, [3]Department Of Computer Science, University of South Florida, [4]Innovatia Medical Systems LLC, Tampa FL
{aalqassi,cacastr3,stsmith7}@mail.usf.edu,{ketterl,richgitlin}@usf.edu, yusun@cse.usf.edu, pete@innovatiamedical.com

Abstract

This paper describes the design, prototype and deployment of a network of wireless Miniature Anchored Robotic Videoscopes for Expedited Laparoscopy (MARVEL). The MARVEL robotic Camera Modules (CMs) remove the need for a dedicated trocar port for an external laparoscope, additional incisions for surgical instrumentation, camera cabling for power, video and xenon light, and an assistant in the operating room to hold and position the laparoscope. The system includes: (1) Multiple MARVEL CMs that feature a wireless controlled pan/tilt camera platform, which provides a full hemisphere field of view inside the abdominal cavity from different angles, wirelessly controlled focus and a wireless illumination control system, (2) a Master Control Module (MCM) that provides a near-zero latency video wireless communications link, independent wireless control for multiple MARVEL CMs, digital zoom, manual focus, and a wireless Human-Machine Interface (HMI) that provides the surgeon with full control over all the functions of the CMs. In-vivo experiments on a porcine subject were carried out to test the performance of the system.

I. Introduction

Laparo-endoscopic Single Site (LESS) Surgery expands upon the minimally invasive properties of laparoscopy and represents a paradigm shift in Minimally Invasive Surgery (MIS) [1]. For most operations, LESS surgery is performed through the umbilicus and, as a result, leaves no discernable scar. Limiting the application of LESS surgery are issues of adequate imaging and access to the peritoneal cavity. Because LESS surgery is undertaken through the umbilicus alone, without additional incisions or trocars distant from the umbilicus, LESS surgery has placed further demands on instrumentation and, especially, imaging. LESS surgery requires an uncluttered operative field with as few instruments as possible transgressing the abdominal wall, through the umbilical port site, as there is only a limited space and a limited number of access points (i.e. trocar sites). In addition to the videoscope (e.g. laparoscope), a typical MIS operation involves the use of multiple instruments, for tasks such as cutting, cauterizing, suctioning, and suturing. The insertion of multiple instruments and the videoscope through the same small incision, at the umbilicus, can lead to mutual interference between instruments, termed 'sword-fighting', which complicates and lengthens the surgical procedure.

It is apparent from the available literature that significant progress has been made in endoscopic technologies. Researchers at Vanderbilt University designed a wired single-port camera that uses an external magnet and a robotic internal active Magnetic Levitation System to produce a precise tilt motion [2]. A device developed by University of Colorado researchers features a single-port camera and an integrated display system that is integrated to a modified custom grasper tool to hold an external display and the internal vision system [4]. Other research by Columbia University [5]-[6], features a camera with low power consumption and high efficiency pan/tilt mechanisms. At the University of Nebraska, Lincoln [7]-[8] work has been done on a robotic camera system that moves through the abdominal cavity while tethered to a supporting cable for power and video interfacing. Finally, recent work at The BioRobotics Institute, Scuola Superiore Sant'Anna, Pisa, Italy [9] resulted in the design of three 12mm diameter modular robotic units: a camera, a retractor and a manipulator unit, and the assembly and testing of a camera unit.

While much progress has been made in endoscopic technology, none of these approaches are ideal for LESS surgery. The current approaches either require additional cabling, which defeats the purpose of single-site surgery, or the proposed scopes are expensive, awkward, bulky or otherwise insufficient for the task. The research described in this paper not only solves these problems, it takes the next step in advancing the MIS paradigm with the design

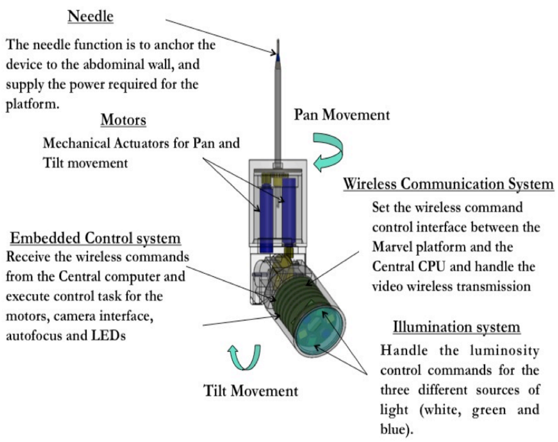

Figure 1:CAD design exploded view of the internal configuration of the *MARVEL* CM.

of a wireless Miniature and Anchored Robotic Videoscope for Expedited Laparoscopy (*MARVEL*) platform [10], which is a cable-free platform placed within the operating cavity prior to surgical procedures. This platform removes any need for additional incisions in the abdomen while providing a clearer view of the operating cavity. It also frees ports in single-site multi-port trocars allowing for greater dexterity to surgeons and insertion of additional surgical tools for safer overall operations. In order to design a reusable Research Platform where new functionality can be added and tested efficiently, a 3x size model was designed, taking care to ensure that the electronics could fit in a 1x (~10mm) commercialized camera module (CM). The 3x MARVEL CM is 105mm long with a diameter of 30mm.The small millimeter-scale and self-contained, cable-free nature of the *MARVEL* CMs will also help alleviate visual depth loss noted when undertaking operations with conventional video instrumentation. Since adding multiple such camera platforms within the body is not constrained by the limited number of incisions or trocar sites, due to their serial insertion, surgeons can add several CMs as space permits within the operating cavity without increasing the overall invasiveness of the procedure and without adding to the clutter of the operative field. Multiple "smart" camera platforms can provide surgeons with additional real-time imaging of a broader operative field, provide visual depth to the image of the operative field, expedite completion of operations, and promote patient safety.

II. System Architecture

The system architecture is comprised of a wireless Human Machine Interface (joystick), a processor-based Master Control Module (MCM), High definition video display, and a wireless Camera Module (CM) anchored to the abdominal wall (Figure 2).

An attachment module (Figure 2) is used to attach the *MARVEL* CMs to the abdominal wall after they are inserted through the single incision used for LESS.

- Master Control Module (MCM):

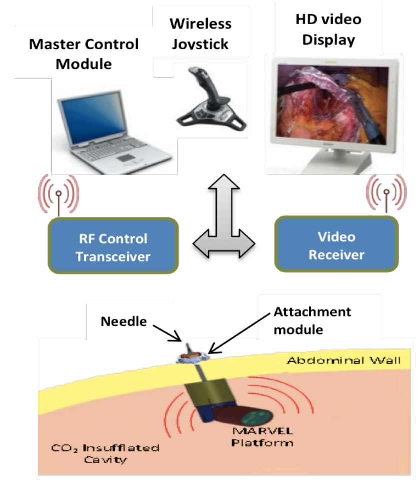

Figure 2: Functional diagram of *MARVEL* Camera Module (CM).

A LabVIEW application processes all the commands coming from the joystick (focus, pan/tilt movement, zoom and light intensity) and sends them via a serial interface to a RF Control/Video Transceiver. A zoom algorithm, which is running in the background, receives zoom in/out commands from the joystick, to format the displayed high definition image on the video monitors.

- Marvel Robotic Camera Module:

A typical *MARVEL* CM (see Figure 3) is comprised of five subsystems: (1) the illumination subsystem provides light to enable clear vision inside the abdominal cavity, (2) the video imaging subsystem provides the optimal focus range and video resolution, (3) the wireless communication subsystem handles the control commands and video between the CM and the MCM, (4) the embedded control subsystem is the management device for the CM, and (5) the needle serves as the anchor mechanism and power source for the CM.

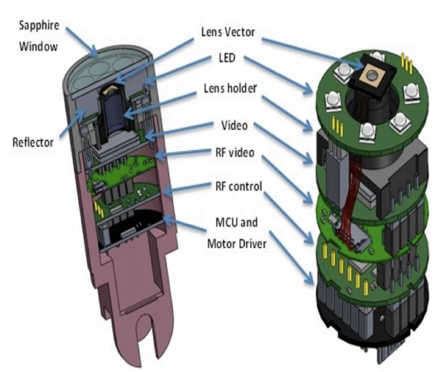

Figure 3: *MARVEL* electronics stack

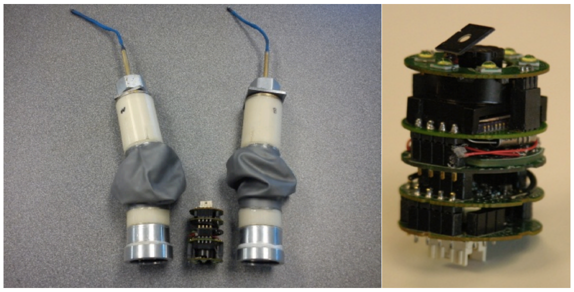

Figure 4. Left: CMs final prototype, Right: PCB stack after assembly.

At the core of the embedded control system is an 8-bit Silicon Lab microcontroller. The MCU provides a Serial Peripheral Interface Bus (SPI) bus to control the SM-band (925 MHz) digital transceiver, an I2C bus to control the video image sensor, and a control interface for the LEDs and pan/tilt motor control lines.

The MCU uses a SPI interface to acquire the wireless data coming from the ISM digital transceiver IC and an I2C interface to control the Liquid Crystal Lens (LCL) driver and the Video Sensor. The motor control commands are implemented by four Pulse Width Modulation (PWM) signals at 24 KHz in direct interface with a H-bridge dual motor driver; the speed of the pan motor can be changed from 0.48 rpm to 31 rpm and the speed of the tilt motor can be changed from 0.24 rpm to 17 rpm, giving the surgeon a very smooth degree of control over the CM. Three GPIO lines are dedicated to control the step-up converter for LED intensity control. Each of the lines carries a PWM signal at 400 Hz.

III. Video Imaging Subsystem

Figure 5 shows the CAD model of the Video Imaging Subsystem, which consists of: (1) a Sunex lens holder that has been customized to fit the system design, (2) a Largan lens with an image format of 12.7” that provides a focal length of 4.37 and focal range between 60mm and 100mm at a maximum of 2M pixels, (3) a LensVector liquid crystal lens (LCL). There is a manual focus capability that can be automated. The focus can be changed from 0 diopters to +10 diopters. The LCL has no motors or moving parts, which makes it easy to integrate with an existing fixed-focus camera modules to add manual focus capability without changing the module footprint [1], (4) and an OmniVision OV7949 video image sensor with a sensitivity of 4.6V/Lux-sec, an imaging array size of 510 x 496 pixels, and a pixel size of 9.2µm x 7.2µm.

The combination of the LensVector liquid crystal lens and the Largan fixed lens extended the focal range of the CM. The Largan Lens was first tested separately on an optical testing bench. The results showed that the lens has limited depth of focus and is unable to focus in close while still being in focus further away. Therefore, the LCL was inserted into the optical path to extend the focal range. The LCL operates by applying a small control voltage that dynamically changes the refractive index to adjust focus to any desired distance from infinity to 10cm. The focus is controlled wirelessly using a joystick as the command unit. The purpose of the LCL is to replace the complex, bulky and often-fragile traditional mechanical auto focus approach of a camera.

The combination of both lenses resulted in a minor increase in the focal range from 70mm- 100mm to 40mm-100mm. The minor increase was due to the fact that the liquid crystal lens only adds up to 10 diopters to the

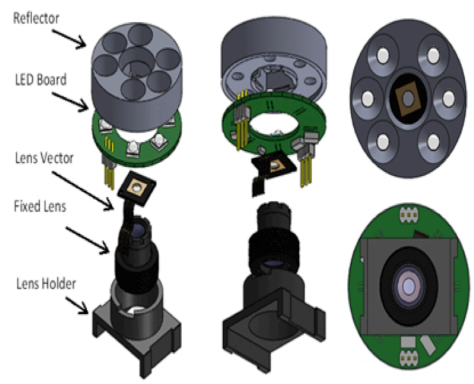

Figure 5: CAD model of the vision system

optical system. Analysis showed that we need a minimum of 40 diopters to achieve the desired depth of field. To calculate the power of a lens needed to focus at a particular distance, we divide 100 by the distance in centimeters. For example, choosing an object that is 2.5cm away, which is what we are targeting: We divide 100 by 2.5 to obtain 40 diopters needed to focus at that particular distance. Below is the formula used:

$$D=100/F \qquad (1)$$

Where D is diopters and F is the focal length (or distance) in centimeters.

Due to the limited depth of field using our current lens arrangement, we have been working with Sunex to design a custom lens that is small enough to be effectively be used in 10mm commercial devices, and has a much greater depth of field. The current CM video imaging subsystem uses a Sunex lens with characteristics much closer to an eventual custom design. Its effective focal length (EFL) is 2.3, aperture (FNO) is 6, and diagonal field of view is 80 degrees.

To evaluate the new Sunex lens, we used an optical test bench to compare the focus range of the Largan and Sunex lenses. An object was placed at multiple distances and an image was captured using each lens separately with the

OV7949 video imaging subsystem. Figure 6 top left shows a resolution chart image at a distance of 60mm using the Largan lens. We have a sharp focused image. Without adjusting the focus, we positioned the resolution chart at a distance of 110mm as seen on the top right. We can note that at the same focus, we were unable to generate a clear focused image of the object placed at a further distance.

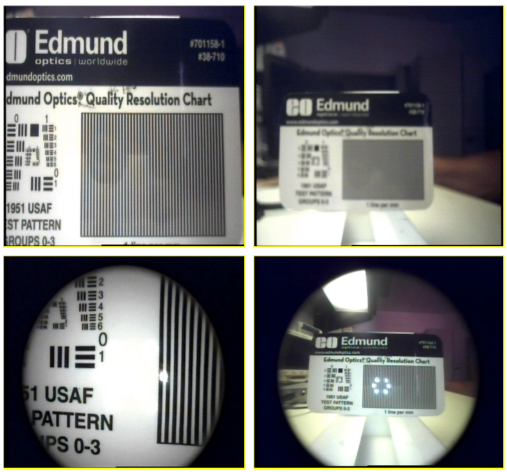

Figure 6. Top Left: Captured images using Largan lens at 60mm, Top Right: Captured image using Largan lens at 110mm. Bottom Left: Captured images using new Sunex lens at 15mm, Bottom Right: Captured image using new

The result demonstrates the need of mechanical "autofocus", which mechanically adjusts the distance of the lens from the imaging sensor to provide a focused sharp image. However, based on our design, the available mechanical autofocus arrangements don't meet the size requirements. Therefore we migrated to using the liquid crystal lens, but since it is limited to 10 diopters of change, a custom lens design was considered. The left bottom of Figure 6 shows an image of the resolution test chart at a distance of 15mm using the new Sunex lens. Without adjusting the focus we placed the chart at a distance of 110mm as seen on the bottom left. The focus and the sharpness were not affected when the chart was positioned at a further distance. This demonstrates the capability of the new Sunex lens. We can note the significant larger depth of field. A custom designed lens would incur significant costs and development time. However, this new lens is an intermediate step toward a custom lens design that would match the parameters of a commercialized CM.

To enhance our video imaging subsystem, we developed software that implements a digital zoom capability. The surgeon can remotely control the digital zoom using the wireless control joystick. During surgery, the surgeon is able see both the original image and the zoomed image displayed on the monitor as seen in Figure 7. This allows the surgeon to work on the zoomed area while still monitoring the outside of the zoomed area in case of an unexpected event.

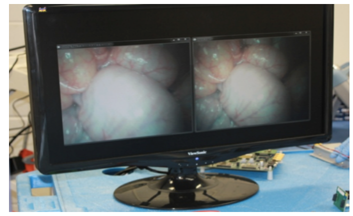

Figure 7. Right: original image, Left: Digital zoom at 20%

IV. Illumination subsystem

The illumination subsystem of each CM consists of an LED board, reflector array, an aluminum heat sink, and Sapphire crystal glass as showing in Figure 8. The LED board is designed with 6 Cree XP-E white LEDs.

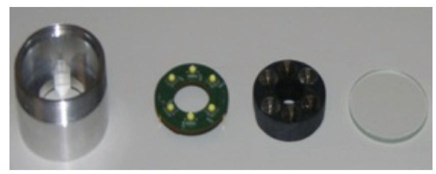

Figure 8: Heat sink, LED board, reflector array and sapphire crystal glass.

The XP-E is a high-efficiency white LED that delivers up to 148 lumens in cool white (6500K) at 1W. At a 150°C junction temperature, the LED efficiency drops by 30%, therefore an aluminum heat sink was designed to keep the junction temperature of each LED below 60°C. Additionally, a Bergquist Sil-Pad thermally conductive insulator is placed under the LED board to efficiently transfer heat from the LEDs to the heat sink. This design is optimized to keep the temperature of the LEDs low since the efficiency of the LEDs is inversely proportional to the junction temperature, and higher temperatures can be dangerous to the patient.

Figure 8 shows the reflector array that was designed to increase illumination efficiency. It maximizes the amount of light that hits the target, increasing the light returning to the video image sensor. Reflectors with half angles of 10, 20, and 30 degrees were tested. A photodiode was used to measure the LED illumination spatial distribution of each reflector.

As can be seen from Figure 9 the intensity falls off as the angle increases. The smaller half- angle cones lead to sharper light distribution patterns. The pattern without the reflector is much flatter and broader than that with the reflector [3]. In this case, we found that 30-degree (half-angle) reflector to be the most effective as we tested the reflectors with a CMOS video image sensor.

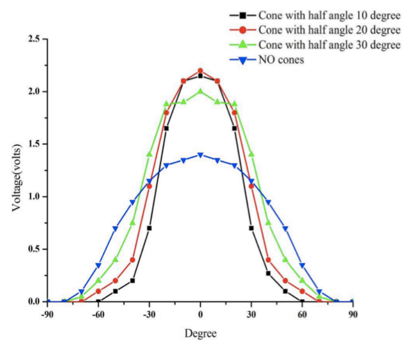

Figure 9: Distribution of light using different cones angles

A Sapphire crystal disk fits on top of the reflector array. Sapphire is used for its extreme surface hardness, high thermal conductivity, and anti-fogging surface.

To enhance our illumination subsystem, we have an intensity control feature that allows the surgeon to wirelessly control the intensity of the LEDs from the joystick.

V. In vivo and RF transmission for wireless Video

Accurate *in vivo* channel models are essential in the development of video image wireless transmission through the human body. Video latency is increased by biological tissues, which are very dispersive to RF signals and can cause signal distortion during video transmission. It is essential that we characterize (RF) signal transmission efficiency through the human body. The *in vivo* channel is very different from the classic multipath communication medium, since the electromagnetic wave is passing through different media that have different electrical properties such as skin, fat, and muscle.

Before implementing and testing the video transmission, we used advanced 3D electromagnetic simulation software, ANSYS HFSS [11], to model how electromagnetic signals propagate through the human body. For *in vivo* channel characterization, a complete human body model is used, with geometric accuracy down to 1mm that completely characterizes the electrical properties of over 300 organs, bones and tissues (Figure 11).

Once the channel characteristics have been derived from simulations, the channel impulse response (CIR) can be calculated. The CIR provides the system response of the channel as a function of time, which can be used in RF system simulators to help design and optimize transceiver systems. For this application, we captured the composite signal from a standard definition video camera with a composite output. The captured signal was used as the drive signal in Ansys' RF circuit and systems simulator Designer [12]. In the simulation, the analog composite signal was FM modulated to carrier frequencies of 1.2 GHz, and transmitted through the *in vivo* channel using the CIR calculated from the HFSS simulation. The channel model was derived from simulations and implemented into our system design to model the video transmission signal. The input and output of the composite signals were compared in the software and it was observed that a very insignificant distortion the in signal quality of the received signal occurred after transmission through the human body in simulation.

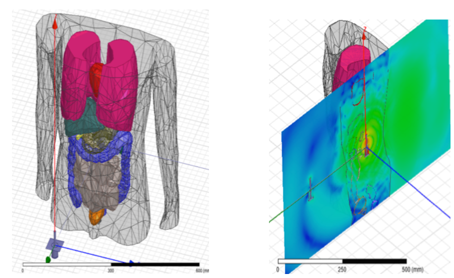

Figure 11. Righ: HFSS Human Body Model showing Major Organs, Left: Simulated Electromagnetic Fields Cut through the Human Body

Figure 12 shows the composite signal with the embedded color burst comparing the transmitted and the received signals. Very little latency (~0.1 us) can be seen in the plot. To enable multiple wireless robotic cameras operating at the same time, each device was designed to transmit at a different modulated frequency. Inexpensive off-the-shelf receivers were used to receive the transmitted video signal and input to a LCD monitor at a near-zero latency. This allows the surgeon to view an extended range of the surgical area in real time. More *in vivo* evaluation and results are described in [10] [12].

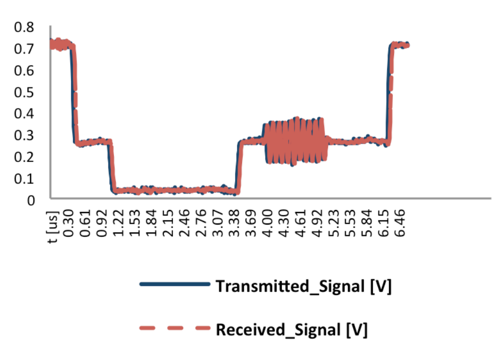

Figure 12: Comparing transmitted composite signal to received signal through the human body simulation

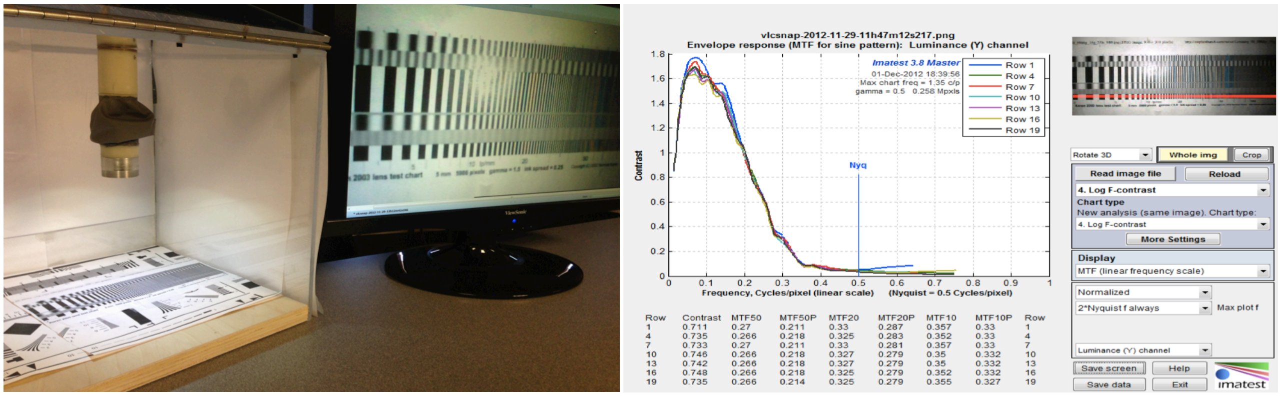

Figure 14. Left: Resolution Test Fixture. Right: Modulation transfer function (MTF), the MARVEL Cm presents a resolution of 0.27 pixels per cycle.

VI. Video Imaging Subsystem Evaluation

To ensure reliability and functionality of the Video Imaging Subsystem, an evaluation test was completed in our lab. The test consisted of three parts: focus at different target positions, digital zoom test, and resolution with sharpness. Two CMs were placed inside a 10x11x16 inch clear plastic. A high quality image of the human body organs was placed inside a phantom model to provide a similar view of the abdominal cavity. The phantom model was placed at multiple different distances ranging from 2 to 6 inches, which is the range required by the surgeon. Figure 13 shows the phantom model placed 3 inches away from the CM. We can observe the difference in the image sharpness as the focus was adjusted.

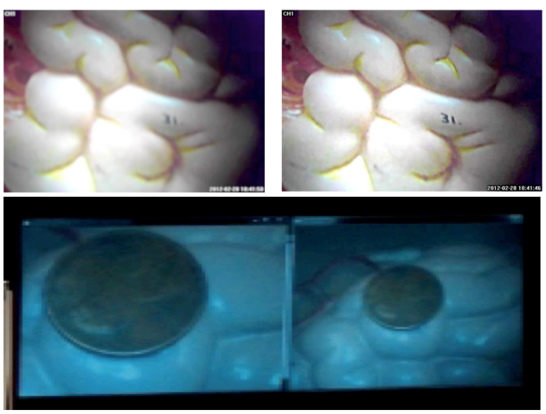
Figure 13. Top Left: Unfocused image, Top Right: focused image, Middle Left: zoomed image at 50%, Middle Right: original image.

Digital zoom testing was also accomplished by placing a penny on top of the intestines to serve as a target. We concluded digital zoom was practical at a maximum of 50%. Beyond this percent zoom we saw a significant loss in image resolution (Figure 13), which shows the importance of migrating to a high definition video.

For the resolution testing, the CM was positioned vertically to a resolution chart so that the resolution chart filled the field of view of the CM (Figure 14); the zoom was set to zero, the focus set to maximize the sharpness of the camera, and the LED light set to 550 lumens at 5000 K color temperature. Figure 14 shows the analysis of the resolution.

VII. Experiment

We have used the imaging system in *in vivo* porcine animal tests. The experiments took place in the USF Vivarium led by experienced laparoscopic team surgeons, Drs. Rosemurgy and Ross. The peritoneal cavity of the animal was insufflated where Two *MARVEL* CMs (Figure 15) and one Olympus laparoscope were inserted prior to starting the test.

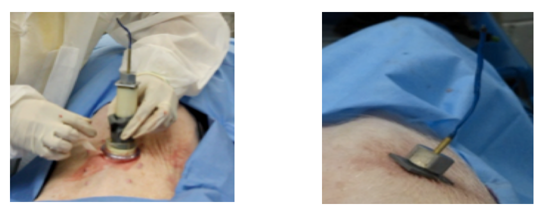
Figure 15. Left: Surgeon inserting CM; Right: attachment module on the coaxial needle securing the CM in place

The surgeon used a trocar to penetrate the abdominal wall and an incision was made to insert the CMs. The surgeon secured the CM in place by putting an attachment module on the coaxial needle as seen in Figure15.

We were able to test the Video Imaging Subsystem, video signal transmission, video quality, CM sealing, and wireless control of the CM. A "balloon" was used to seal the open area between the tilt and pan cylinders.

The surgeon was able to observe the abdominal cavity by controlling the two CMs wirelessly using the joystick. He was able to extend the view of the surgical area by position both CMs to view side by side (Figure 16).

The surgeon also tested the wireless manual focus. He was able to change the focus wirelessly using the joystick. This gives the surgeon the ability to enhance the image visibility in areas that requires further detail. Focus range was between 2 to 6 inches as expected from the evaluation test. Figure 16 bottom shows the capability of the manual focus.

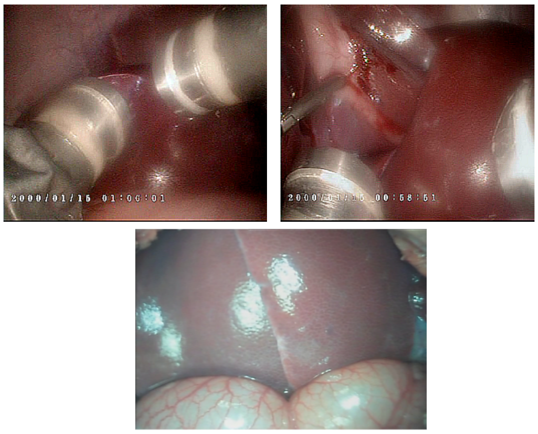

Figure 16. Top: *MARVEL* CMs inside the porcine abdominal cavity. Bottom: Image of porcine intestines and liver taken by a MARVEL CM using manual focus feature.

Zoom functionality was a success. Figure 17 shows the original image and the zoomed image at 50% captured during the experiments.

The result from illumination system was as expected. An improved future illumination system would include RGB combination for creating true white color at a different temperature between 4000 and 6500 kelvin. This will allow doctors to clearly distinguish different organs and tissue structure, and preferably to some extent, as needed color temperature adjustment, to highlight a certain organ or tissue [13].

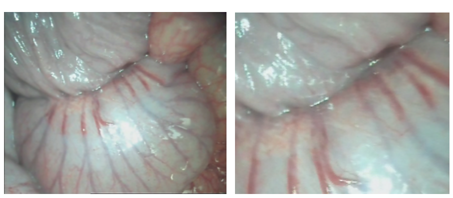

Figure 17. Left: original image, Right: Digital zoom at 50%

VII. Conclusion and Future Work

Two robotic camera modules were tested at the University of South Florida College of Medicine. The result of the laboratory experiments shows the importance of migrating to a high definition wireless video in order to increase video quality, focus, and digital zoom. It also shows the importance of optimizing a network robotic endoscopic system that will significantly advance the field of minimally invasive surgery. Integrating a mesh network for communication between multiple robotic CMs will be a unique step for the next devices using ZigBee communications protocol. In addition, extending the range of view from the camera by using pixel edge matching algorithm that would allow multiple images from multiple CMs to create panoramic video display of the surgical site would be also a future design.

References

[1] Romanelli JR, Earle DB, Single-port laparoscopic surgery: an overview. Surgical Endoscopy 2009 Jul; 1419-1427.

[2] M. Simi, M. Silvestri, C. Cavallotti, M. Vatteroni, P. Valdastri, A. Menciassi, P. Dario, “Magnetically Activated Stereoscopic Vision System for Laparoendoscopic Single Site Surgery”, IEEE Transactions on Mechatronics, 2012.

[3] P. Berkelman, P. Cinquin, J. Troccaz, J. Ayoubi, C. Letoublon, and F. Bouchard. “A compact, compliant laparoscopic endoscope manipulator,” In IEEE Intl. Conf. on Robotics and Automation, pages 1870–1875, 2002.

[4] Terry, B.S., Ruppert, A.D., Steinhaus, K.R., Schoen, J.A., Rentschler, M.E., “An Integrated Port Camera and Display System for Laparoscopy,” *IEEE Transactions on Biomedical Engineering*. 57(5): 1191-1197, 2010.

[5] T. Hu, P. K. Allen, N. J. Hogle, and D. L. Fowler. Insertable surgical imaging device with pan, tilt, zoom and lighting. In International Conference on Robotics and Automation (ICRA), May 19-23 2008.

[6] T. Hu, P. K. Allen, T. Nadkarni, N. J. Hogle, D. L. Fowler, "Insertable Stereoscopic 3D Surgical Imaging Device with Pan and Tilt," in IEEE / RAS-EMBS International Conference on Biomedical Robotics and Biomechatronics (BIOROB), Scottsdale, AZ, USA, 2008, pp. 311-316.

[7] Platt, S. R. Vision and task assistance using modular wireless in vivo surgical robots. IEEE Trans Biomed Eng 56:1700-10. 2009.

[8] Hawks, J., Rentschler, M., Redden, L., Infanger, R., Dumpert, J.,Farritor, S., Oleynikov, D., & Platt, S. (2008). Towards an in vivo wireless mobile robot for surgical assistance. Studies in Health Technology and Informatics, 132,153-158.

[9] G. Tortora, A. Dimitracopoulos, P. Valdastri, A. Menciassi, P. Dario, “Design of Miniature Modular in vivo Robots for Dedicated Tasks in Minimally Invasive Surgery”, 2011 IEEE/ASME International Conference on Advanced Intelligent Mechatronics (AIM2011).

[10] Castro, C. A.; Smith, S.; Alqassis, A.; Ketterl, T.; Sun, Y.; Ross, S.; Rosemurgy, A.; Gitlin, R. D. “MARVEL: A Wireless Miniature Anchored Robotic Videoscope for Expedited Laparoscopy,” In 2012 IEEE International Conference on Robotics and Automation (ICRA 2012).

[11] “ANSYS HFSS.” [Online]. Available: http://www.ansoft.com/products/hf/hfss/. [Acc: 11/22/11].

[12] T. P. Ketterl, G. E. Arrobo, A. Sahin, T. J. Tillman, H. Arslan, and R. D. Gitlin, "*In Vivo* Wireless Communication Channels," IEEE 13th Annual Wireless and Microwave Technology Conference (WAMICON) 2012, pp. 1-3

[13] Nathaniel J. Soper, Lee L. Swanström, W. Stephen Eubanks, Mastery of endoscopic and laparoscopic surgery. Lippincott Williams & Wilkins 2009, ch. 3.